Research Article
cnj.araku.ac.ir

☑ Cite This: Colloid Nanosci. J. 3(4) (2025) 768-774 DOI: 10.66224/CNJ.3.4.768

Diphenylamine-based Colloidal Graphene Quantum Dots with Enhanced Blue-emission

Reza Sahraei1*, Leila Omidi1, Ehsan Soheyli2

1 Department of Chemistry, Faculty of Science, Ilam University, Ilam, Iran
2 Department of Physics, Faculty of Science, Ilam University, Ilam, Iran

ARTICLE INFO

Article History:
Received: 2025-12-02
Revised: 2025-12-11
Accepted: 2025-12-12
Published: 2025-12-16

Corresponding Authors:
Reza Sahraei
Email:
sahraei.r@gmail.com

ABSTRACT

Representing new precursors to achieve enhanced emission properties in carbon-based quantum dots is a promising academic task. In the present study, deep-blue emissive graphene quantum dots (GQDs) were successfully synthesized through a facile one-step solvothermal treatment using diphenylamine and formamide as precursors, demonstrating an efficient molecular-carbonization strategy for producing highly luminescent carbon nanomaterials. In this approach, diphenylamine served mainly as the carbon source, while formamide plays the role of dopant precursor, enabling controlled heteroatom incorporation during the nucleation and growth of sp^2-dominated graphene domains. The solvothermal reaction promoted oxidative dehydrogenation and polymerization of the aromatic precursor, followed by gradual carbonization to yield GQDs with broad emission signal located at around 398 nm. Structural characterization revealed the presence of carbon/oxygen/ and nitrogen elements, along with abundant surface functional groups, including amine, hydroxyl, and carboxyl moieties that ensured excellent water dispersibility and contributed to bright photoluminescent behavior. The combined simplicity of the synthetic process, the use of an inexpensive aromatic precursor, and the favorable optical characteristics with emission quantum efficiency of 56.6% underscore the potential of diphenylamine-derived GQDs as versatile nanophotonic materials for sensing, light-emitting devices, and fluorescence-based diagnostics.

KEYWORDS: *Graphene quantum dots, Diphenylamine, Solvothermal, Deep blue emission*

1. Introduction

Luminescent artificial materials are fascinating species that actively develop to realize the demands of industry in optoelectronics, sensing, anticounterfeiting, and bioimaging. Carbon dots (CDs) are nascent zero-dimensional carbon-based nanostructures with flourishing applications in the past decade. They are luminescent nanomaterials composed of sp2/sp3 hybrids as carbon cores enriched with surface functional groups, that endow them a research hotspot in various fields of bioimaging, optoelectronics, and sensing [1,2]. Fundamentally, they are able to show high photoluminescence quantum efficiency (PLQYs), adjustable light emission wavelengths, and excellent photostability that are accessible via various preparation techniques. Indeed, a broad range of precursors, including plant-based extracts [3], amino acids [4,5], polymers [6], aromatic molecules [7], and other organic compounds such as egg shell [8], and fruit-juice [9] represents a tremendous possibility for preparing CDs. Besides, they can be prepared with different names and properties such as carbon nanodots (CNDs), carbon quantum dots (CQDs), graphene quantum dots (GQDs), and carbon polymer dots (CPDs) [10]. The difference mainly depends on the precursors used and the crystalline structure. For example, CNDs are known for their short-ordered amorphous structure, while GQDs show enhanced crystallinity. In our previous study, tiny CNDs with short-range atomic order and bright blue emission at 420 nm was prepared using tri-sodium citrate

as the main carbon source and N-acetyl-l-cysteine (NAC) as a dopant source [11]. They were prepared via microwave method and photoluminescence (PL) emission intensity was optimized at different reaction conditions to reach PLQY of 62%. Doped-CDs were then employed in fingerprint detection. In another report, a low-cost amino acid was used to react with urea and 1-octhanethiol through solvothermal heating method and blue emissive GQDs with PLQY of around 70% was achieved [12]. They showed three recombination pathways with average excited-state lifetime of 2.4 ns. Kevser et al. also used boric acid to embed CDs within borate matrix through vacuum-assisted technique [13]. Their composite showed %18 solid-state PLQY at around 450 nm with bi-exponential fitting of recombination process. Microwave-assisted heating via domestic instrument usually suffers from limited access to other solvents except aqueous medium, and the professional microwave system is expensive. Also, the vacuum-based system usually requires an oxygen-free medium commonly known as Schlenk line-set up, which is considered as complicated method. However, simultaneous creation of high pressures and temperatures represents autoclave-assisted heating methods as an easy, straight-forward, and low-cost approach to obtain CDs via various precursors in almost any reaction solvent.

The current study proposes deep-blue emissive GQDs prepared via facile solvothermal method and optimization of experimental variables to reach the best emission features. Formamide and aromatic molecules of diphenylamine (DPA) were ultrasonically dispersed in ethanol (EtOH) and subjected to solvothermal heating for a desired reaction time. The optimized N-doped GQDs revealed an excitation-dependent PL profile with bright signal at around 390-400 nm. Combination of low-cost preparation method, low-toxicity of precursors, and high emission intensity of the prepared GQDs nominate them as excellent candidate for fingerprint sensing, anti-inflammatory.

2. Materials and Methods

All the chemicals including DPA, absolute EtOH, and formamide were purchased from Merck company. A solvothermal heating method was used to react DPA and formamide in EtOH, forming luminescent GQDs. Typically, 0.17 g of DPA was fully dissolved in 10 mL EtOH. After that, 1 mL of formamide was added and stirred to obtain a homogenous solution. Then, it was poured to a 50 mL Teflon-lined autoclave and sealed properly, followed by 14 h of heating at 150 °C in an oven. Finally, the reactor cooled down naturally to room temperature. The as-prepared colloidal solution was quite concentrated with orangish transparent color. It was filtered and centrifuged at 4000 rpm / 10 min to get rid of byproducts (Scheme 1). To perform PLE/PL measurements, 1 mL of this solution was redispersed in 4 mL EtOH. The experimental parameters were optimized in order to reach the best PL emission intensities. The details have been mentioned in Table 1.

Crystalline structure and phase composition were examined by X-ray diffraction (XRD) using a Bruker D8 Discover system. Functional groups and surface chemical bonding configurations were analyzed through Fourier-transform infrared (FTIR) spectroscopy employing a Bruker Vertex instrument. Elemental compositionwas determined by energy-dispersive X-ray (EDX) spectroscopy with an Oxford 7538 detector. Morphological features and particle size distribution were investigated via transmission electron microscopy (TEM) using a JSM-6700F operated at 200 kV. Optical absorption characteristics were recorded using UV–visible spectroscopy on a Cary 300 Bio spectrophotometer. Photoluminescence excitation (PLE) and emission (PL) spectra were obtained with a Cary Eclipse system. Collectively, these complementary analytical techniques enabled

Table 1: The details of experimental parameters used to reach optimized PL emission results

	DPA (mmol)	Formamide (mL)	Reaction Temp. (°C)	Reaction Time (h)	EtOH (mL)
1	0.5 – 1 – 2	1	150	14	10
2	1	0.5 – 1 – 1.5 – 2 – 2.5	150	14	10
3	1	1.5	150	8 – 14 – 20 – 24	10
4	1	1.5	120 – 150 – 180	14	10

Scheme 1: Schematic representation of preparation method.

a comprehensive evaluation of the structural, chemical, morphological, and optical properties of the prepared GQDs.

3. Results and Discussion

Direct observation of the prepared GQDs was realized via TEM analysis where tiny spherical-type particles with average sizes of 3.6 nm were detected (Fig. 1A). XRD patterns of the samples, prepared at different reaction temperatures, plotted in Fig. 1B. All showed sharp peaks at 2theta values around 9°, 13.8°, and 18.6°. They are mainly related to the (001), (100), and (002) Miller index of graphene oxide [14–16].

To determine the constituent elements of the prepared GQDs, EDX analysis was performed for GQDs prepared with different amounts of DPA. As shown in Fig. 2, around 74-83 atomic percent of the GQDs structure belongs to carbon. Since the DPA precursor consists of two phenyl rings attached to an amine group, after increasing the amount of DPA from 0.5 to 1, and then 2 mmol, the amount of carbon and nitrogen increased while the oxygen level decreased.

Fig. 3 illustrates the FTIR spectra of GQDs prepared at different reaction times. The broad and intense peaks at 3100-3600 cm^{-1} are attributed to the O-H and N-H stretching vibrations. Well-resolved tiny peaks at 2800 and 2900 cm^{-1} belong to symmetric and asymmetric CH_2 stretching vibrations while the C-H bending vibrations appeared at 1480 cm^{-1}. The strong peak at 1700 cm^{-1} represents the C=O vibrations. The graphitic domain of the prepared GQDs was observed at

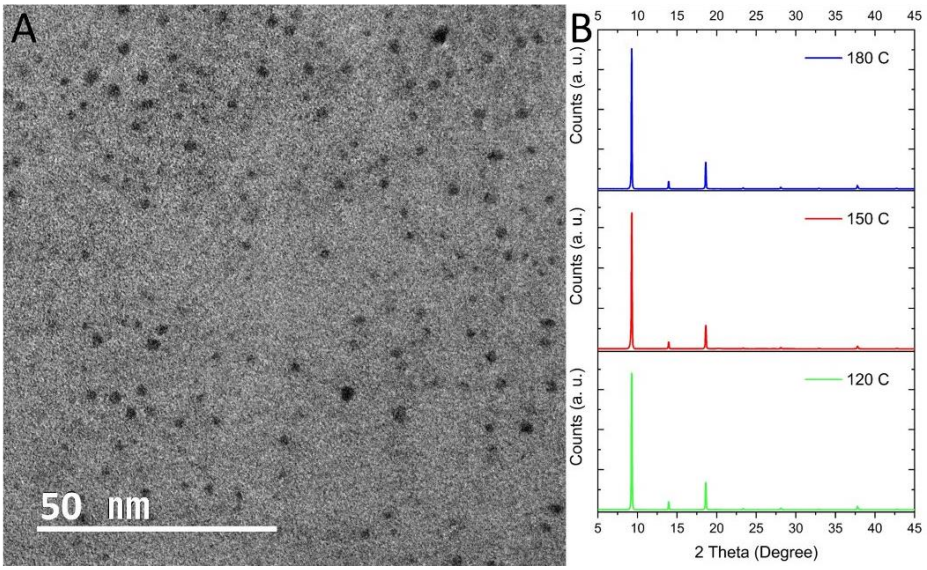

Fig. 1: A) TEM image of the sample prepared at 150° for 14 h of reaction time. B) XRD patterns of samples prepared at different reaction times of 120°, 150°, and 180°.

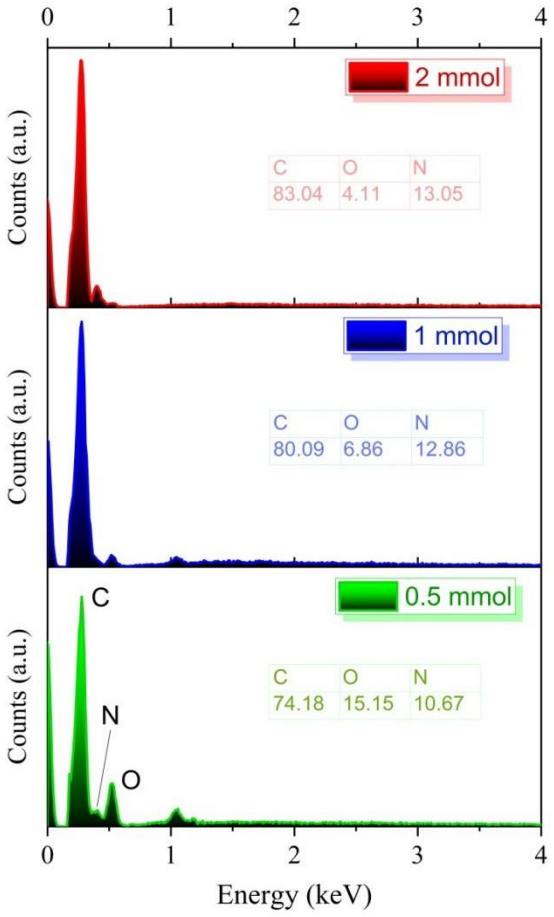

Fig. 2: EDX spectra of the prepared GQDs with different amounts of DPA in the presence of 1 mL formamide at 150° for 14 h of reaction time. The corresponding atomic percent of the constituent elements.

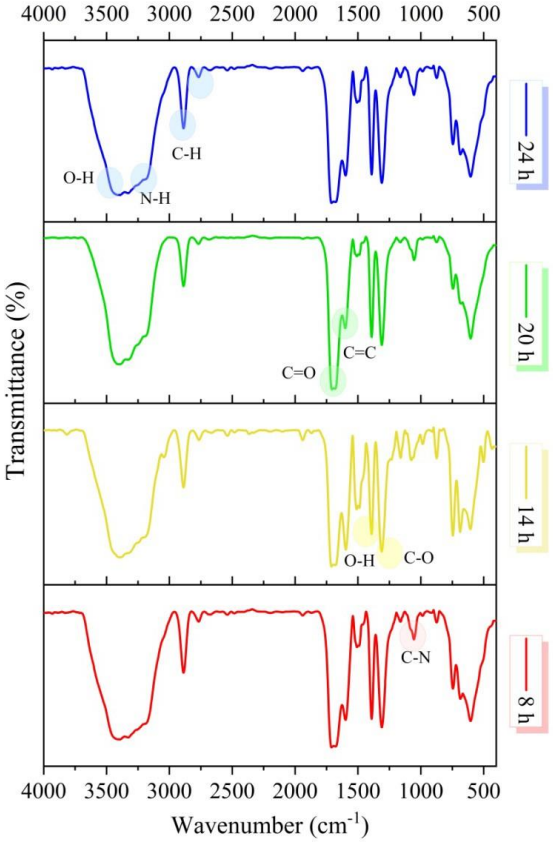

Fig. 3: FTIR spectra of the prepared GQDs at different reaction times in the presence of 1 mmol DPA, 1.5 mL formamide under reaction temperature of 150°.

around 1600 cm^{-1} related to the C=C cycloalkene vibration groups. The carboxylic acid-related bending vibrations of O-H was also appeared at 1400 cm^{-1} and stretching vibrations of C-O emerged at 1300 cm^{-1}. The weak peak appeared at 1080 cm^{-1} indicates the formation of stretching vibrations of C-N. These results support the existence of enriched surface functional groups.

Generally, carbon-based quantum dots are well-known in optoelectronic devices and biophotonics. To do so, they should represent a bright emission. Here, the effect of experimental parameters is evaluated on optical properties of the prepared GQDs as summarized in Table 1. Initially, the excitation-dependence PL emission spectra were recorded (Fig. 4). Results showed a variable PL peak positions from 378 nm to 465 nm, while the intensity of emission profile change remarkably. The highest intensity was obtained for excitation wavelength of 340 nm.

Using the various amount of DPA, it was confirmed that PLE plots show an excitation signal at around 345 nm, while the wide PL emission plots were located at around 398 nm (Fig. 5A). The best emission result was recorded for 1 mmol of DPA, where a bright deep blue emission was observed under 365 nm UV-light (inset of Fig. 5A). The same results were concluded at different amounts of formamide, demonstrating that GQDs prepared at 1.5 mL of formamide exhibit a better PL intensity (Fig. 5B). As nitrogen-oxygen precursor, formamide may assist in formation of amin and carbonyl functional groups attached to the surface of GQDs. They act as midgap energy levels to contribute in the formation of radiative centers for excited charge carriers [17]. The reaction temperature was another parameter evaluated here (Fig. 5C). Upon increase from 120 °C to 180 °C, a detectable shift

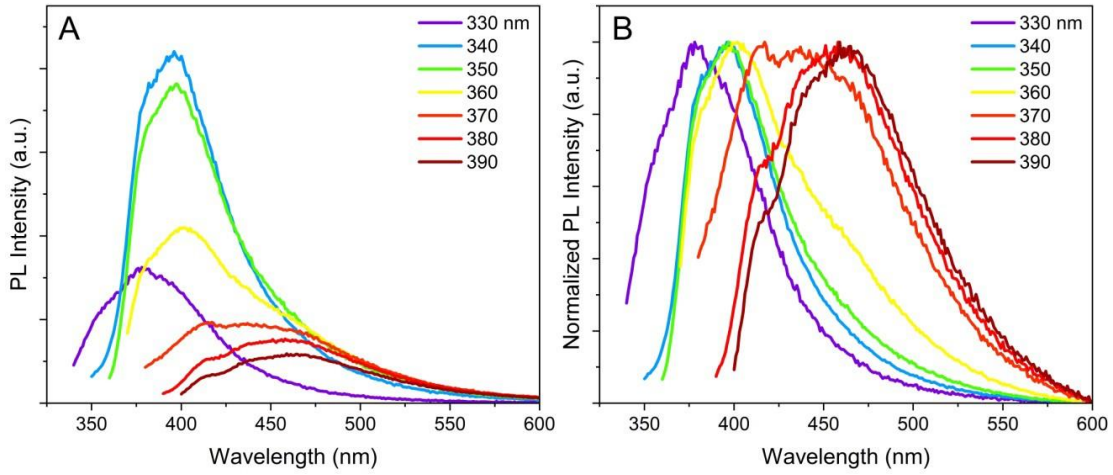

Fig. 4: A) Excitation-dependence PL emission profiles of the GQDs, and B) their corresponding normalized PL plots.

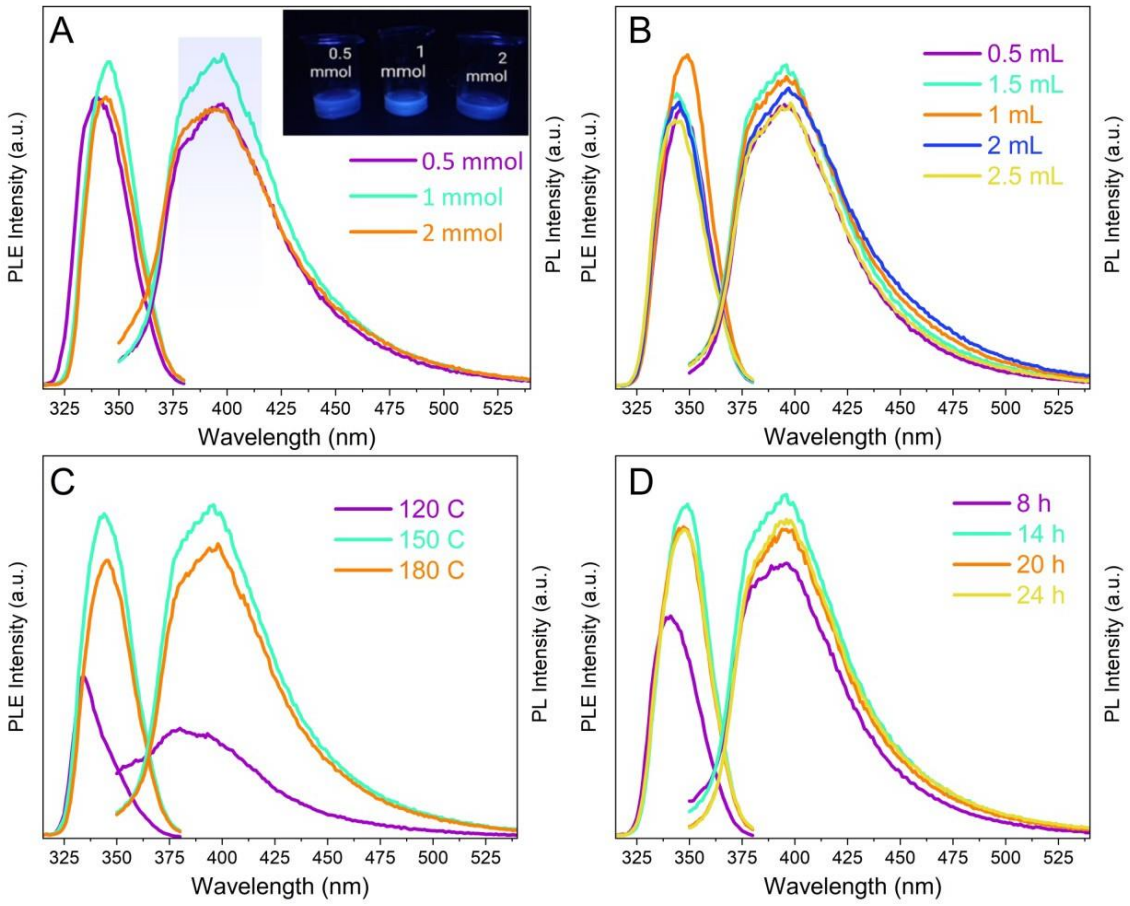

Fig. 5: PLE (λ_{em}=400 nm) and PL spectra (λ_{exc}=350 nm) of GQDs prepared at different; A) amounts of DPA (Inset shows digital images of GQDs dispersed in EtOH, under 365 nm UV-lamp), B) amounts of formamide, C) reaction temperatures, and D) reaction times.

in PLE and PL spectra was recorded toward longer wavelengths, due to possible increase in the size of conjugated carbonized region. The best emission intensity was obtained for GQDs prepared at 150 °C. Finally, the reaction-time's effect on optical properties was evaluated. As shown in Fig. 5D, short reaction time of 8 h results in a lower intensity, while further increase to up to 24 h supports an enhanced emission intensity. The best emission intensity was obtained for GQDs prepared for 14 h. The PLQY of the synthesized sample was determined using the comparative method, in which the emission characteristics of the target material are evaluated against those of a well-established reference fluorophore. In this approach, a standard dye with known quantum efficiency serves as the calibration benchmark for quantifying the radiative performance of the unknown sample. For this purpose, 9,10-Diphenylanthracene was employed as the reference material. This compound exhibits characteristic blue emission maxima at 406 nm and 427 nm, rendering it particularly suitable for comparison with deep blue-emissive nanoparticles. The reported PLQY of 9,10-diphenylanthracene under standard conditions is 95%, which provides a reliable basis for relative quantum yield determination. The PLQY of the sample (ϕ) was calculated according to the established comparative expression of; $\phi/\phi_R=[I/I_R\times A_R/A\times(n/n_R)^2]$, where ϕ and ϕ_R denote the photoluminescence quantum yields of the sample and the reference dye, respectively. The terms I and I_R correspond to the integrated emission intensities obtained from the photoluminescence spectra of the sample and reference. A and A_R represent the absorbance values at the selected excitation wavelength for the sample and reference, respectively. The parameters n and n_R indicate the refractive indices of the solvents used for dissolving the sample and the reference dye. To minimize reabsorption and inner-filter effects, both the sample and the reference solutions were prepared in diluted form. The excitation wavelength was selected based on the intersection point of the absorption spectra of the carbon dots and the reference dye, which occurred at 345 nm. At this wavelength, the absorbance ratio satisfied $A_R/A=1$, thereby eliminating the need for further absorbance correction in the calculation. Consequently, 345 nm was employed as the excitation wavelength for all PLQY measurements to ensure consistency and analytical accuracy. Using the above plots and formula, the PLQY of the optimized GQDs was estimated to be around 56.6%.

4. Conclusion

In summary, this study proposes diphenylamine as a proper carbon backbone to prepare small sized GQDs of about 3.6 nm with short-wavelength emission and excitation-dependent broad PL profile from 378 nm to 465 nm. The dark blue emission at around 400 nm (λ_{exc}=340 nm) was further optimized to realize best emission intensity where the best one obtained for GQDs prepared via 1 mmol DPA, and 1.5 mL formamide during the 14 h of reaction at 150 °C with PLQY of 56.6%. Enriched surface cites via C-O, C=O, N-H, etc groups further confirmed the formation of functional GQDs which highlights their suitability in optoelectronics and nanobiophotonics.

References

[1] M. Alafeef, I. Srivastava, T. Aditya, D. Pan, Carbon Dots: From Synthesis to Unraveling the Fluorescence Mechanism, Small 20 (2024) 2303937. https://doi.org/10.1002/smll.202303937

[2] F. Yan, S. Li, R. Tong, Y. Wang, Y. Fu, L. Chen, Review of Phosphorescent Carbon Dots and Their Applications, ACS Appl. Nano Mater. 8 (2025) 3709–3725. https://doi.org/10.1021/acsanm.4c06540

[3] A. Rezaei, R. Monfared-Hajishirkiaee, S. Hosseinzadeh-Moghaddam, M. Behzadi, S.S. Shahangian, Enhancing leachate management with antibacterial nanocomposites incorporating plant-based carbon dots and Satureja Khuzestanica essential oils, Colloids and Surfaces B: Bio-interfaces 245 (2025) 114296. https://doi.org/10.1016/j.colsurfb.2024.114296

[4] K. Sahin Tiras, A. Biçer, E. Soheyli, E. Mutlugun, Spectrally Tunable White Light-Emitting Diodes Based on Carbon Quantum Dot-Doped Poly(N -vinylcarbazole) Composites, ACS Appl. Nano Mater. 7 (2024) 2744–2752. https://doi.org/10.1021/acsanm.3c04915

[5] N. Sahiner, S.S. Suner, M. Sahiner, C. Silan, Nitrogen and Sulfur Doped Carbon Dots from Amino Acids for Potential Biomedical Applications, J Fluoresc 29 (2019) 1191–1200. https://doi.org/10.1007/s10895-019-02431-y

[6] S. Tao, S. Zhu, T. Feng, C. Xia, Y. Song, B. Yang, The polymeric characteristics and pho-toluminescence mechanism in polymer carbon dots: A review, Materials Today Chemistry 6 (2017) 13–25. https://doi.org/10.1016/j.mtchem.2017.09.001

[7] S. Xue, P. Li, L. Sun, L. An, D. Qu, X. Wang, Z. Sun, The Formation Process and Mech-anism of Carbon Dots Prepared from Aromatic Compounds as Precursors: A Review, Small 19 (2023) 2206180. https://doi.org/10.1002/smll.202206180

[8] Y. Deng, C. Shen, W. Zhao, G. Zheng, F. Jiao, Q. Lou, K.

Liu, C.-X. Shan, L. Dong, Bio-synthesis of the Narrowband Deep-Red Emissive Carbon Nanodots from Eggshells, ACS Sus-tainable Chem. Eng. 11 (2023) 6535–6544. https://doi.org/10.1021/acssuschemeng.2c06892

[9] N. Selvaraju, P.S. Ganesh, V. Palrasu, G. Venugopal, V. Mariappan, Evaluation of Anti-microbial and Antibiofilm Activity of Citrus medica Fruit Juice Based Carbon Dots against Pseudomonas aeruginosa, ACS Omega 7 (2022) 36227–36234. https://doi.org/10.1021/acsomega.2c03465

[10] Y. Liu, Z. Huang, X. Wang, Y. Hao, J. Yang, H. Wang, S. Qu, Recent Advances in Highly Luminescent Carbon Dots, Adv Funct Materials 35 (2025) 2420587. https://doi.org/10.1002/adfm.202420587

[11] S. Savaedi, E. Soheyli, G. Zheng, Q. Lou, R. Sahraei, C. Shan, Excitation-independent deep-blue emitting carbon dots with 62% emission quantum efficiency and monoexponential decay profile for high-resolution fingerprint identification, Nanotechnology 33 (2022) 445601. https://doi.org/10.1088/1361-6528/ac7c27

[12] K.S. Tiras, E. Soheyli, Z. Sharifirad, E. Mutlugun, Optimization of high efficiency blue emissive N-, S-doped graphene quantum dots, Optical Materials 159 (2025) 116544. https://doi.org/10.1016/j.optmat.2024.116544

[13] H. Altintas, K. Sahin Tiras, Vacuum-Assisted Synthesis of Solid-State Fluorescent Car-bon Quantum Dots for Color Conversion LEDs, ACS Omega 10 (2025) 15654–15662. https://doi.org/10.1021/acsomega.5c01047

[14] D.K. Kumar, D. Suazo-Davila, D. García-Torres, N.P. Cook, A. Ivaturi, M.-H. Hsu, A.A. Martí, C.R. Cabrera, B. Chen, N. Bennett, H.M. Upadhyaya, Low-temperature titania-graphene quantum dots paste for flexible dye-sensitised solar cell applications, Electrochimica Acta 305 (2019) 278–284. https://doi.org/10.1016/j.electacta.2019.03.040

[15] Isha, Aneesha, M.S. Mehata, Synthesis of Graphene Quantum Dots (GQDs) from Paddy Straw for Bilirubin Detection, Plasmonics 20 (2024) 2359–2366. https://doi.org/10.1007/s11468-024-02396-0

[16] M. Buldu-Akturk, M. Toufani, A. Tufani, E. Erdem, ZnO and reduced graphene oxide electrodes for all-in-one supercapacitor devices, Nanoscale 14 (2022) 3269–3278. https://doi.org/10.1039/D2NR00018K

[17] N. Havasi, R. Sahraei, E. Soheyli, Y. Lan, Q. Lou, F. Houshmand, G. Zheng, R. Phul, E. Mutlugun, C.-X. Shan, Bright green and blue solid-state emitting carbon dots with optimized photoluminescence characteristics for fabrication of high-performance light emitting diodes, Ceramics International 51 (2025) 38508–38517. https://doi.org/10.1016/j.ceramint.2025.06.086